RESEARCH ARTICLE

Investigation on the Mechanism of Nebulized Droplet Particle Size Impact in Precision Plant Protection

Hui Ma[1], **Jiajia Tang**[1], **Huimin Lv**[1], **Wenyan Chu**[2,*] **and Shengdi Sun**[1]

[1] Valve Intelligent Equipment Engineering Research Center, Department of Mechanical and Electrical Engineering, HeBei Vocational University of Technology and Engineering, Xingtai 054035, China
[2] Department of Electrical Engineering, HeBei Vocational University of Technology and Engineering, Xingtai 054035, China

Abstract

This paper presents an AI-driven intelligent control system for precision spray applications that integrates real-time perception, neural network prediction, reinforcement learning optimization, and online Bayesian learning. A two-tier architecture is established: Tier 1 employs neural network-based feedback control for rapid pressure adjustment (0.1–0.3 MPa), while Tier 2 deploys an RL agent for optimal nozzle selection when pressure control is insufficient. The neural network model achieves high prediction accuracy with an RMSE of 3.2 μm on the test set. The RL agent demonstrates effective decision-making, attaining a 94.5% success rate in simulation and closed-loop experiments for maintaining target droplet size within $\pm$10 μm. Online Bayesian updates improve prediction accuracy by an average of 8.7% after every 100 field observations. Experimental validation demonstrates autonomous optimization, rapid convergence (3–5 cycles), and continuous learning without human retraining, offering a fully autonomous solution suitable for UAV deployment and precision agriculture.

Keywords: neural networks, reinforcement learning, intelligent control, real-time optimization, autonomous systems, precision agriculture.

1 Introduction

Real-time autonomous systems face a fundamental challenge: how to maintain precise control over output characteristics in dynamic, multi-parameter environments without continuous human intervention. This challenge is particularly acute in applications where parameter spaces are high-dimensional and environmental conditions vary unpredictably. Contemporary approaches typically rely on either offline parameter optimization or simple feedback loops, but lack the integrated intelligence to adapt, learn, and optimize across multiple objectives simultaneously. The deposition pattern of spray droplets in plant protection is critical for pesticide efficacy. Research on the deposition law of spray droplet groups, including multiphase flow simulation analysis, provides essential guidance for optimizing atomization parameters to achieve uniform coverage and minimize environmental loss [1].

Academic Editor:
Quanmin Zhu

Submitted: 09 September 2024
Accepted: 26 September 2024
Published: 29 September 2024

Vol. 1, **No.** 2, 2024.
10.62762/TIS.2024.307219

***Corresponding author:**
✉ Wenyan Chu
chuwenyan@xpc.edu.cn

Citation
Ma, H., Tang, J., Lv, H., Chu, W., & Sun, S. (2024). Investigation on the Mechanism of Nebulized Droplet Particle Size Impact in Precision Plant Protection. *ICCK Transactions on Intelligent Systematics*, 1(2), 102–111.

© 2024 ICCK (Institute of Central Computation and Knowledge)

Precision spray application in plant protection requires balancing multiple objectives: (1) maintaining target droplet size for biological efficacy, (2) minimizing pesticide consumption, (3) reducing spray drift, and (4) adapting to diverse crop types and environmental conditions [2]. Traditional systems rely on fixed parameters or operator experience, lacking real-time adaptation. While prior research has characterized offline relationships between nozzle design, pressure, and droplet size, no integrated closed-loop intelligent control system exists. The critical challenge is that smaller droplets provide better coverage and sedimentation but suffer increased evaporation and drift, resulting in pesticide waste. Optimal spray parameter settings must balance these competing effects.

The research gap can be precisely defined across three dimensions: (1) Most prior work characterizes spray parameters through offline experiments or CFD simulations, generating static parameter databases. The challenge of real-time droplet size regulation—maintaining target specifications despite continuous environmental variation—remains unaddressed in the literature. (2) Parameter selection currently relies on lookup tables (deterministic), linear regression models (simple statistics), or operator judgment (heuristic). The gap is the absence of a data-driven, adaptive decision system that accounts for multi-variate environmental inputs and produces environment-aware parameter recommendations with quantified confidence levels. (3) Agricultural systems operate iteratively over extended seasons. The critical gap is the lack of an online learning mechanism that automatically improves model performance based on accumulated field data without human intervention or model retraining by specialists.

To close these gaps, this paper proposes an AI-driven intelligent control system that integrates real-time perception [12], neural network (NN) prediction [8], reinforcement learning (RL) optimization [9, 10], and online Bayesian learning [11]. A two-tier hierarchical architecture is established: Tier 1 employs an NN-based feedback controller for rapid spray pressure adjustment within the operational range of 0.1–0.3 MPa, while Tier 2 deploys an RL agent for optimal nozzle selection when pressure regulation alone is insufficient. The framework enables autonomous parameter optimization, rapid adaptation to dynamic environmental conditions, and continuous model refinement through online learning without human retraining, providing a fully autonomous and scalable solution suitable for UAV deployment in precision plant protection.

The remainder of this paper is organized as follows: Section 2 reviews the related work. Section 3 describes the materials and experimental methods. Section 4 presents the proposed AI-driven system architecture. Section 5 introduces the theoretical basis of droplet atomization and related models. Section 6 reports the experimental results and discussion. The paper concludes with a summary and future research directions.

2 Related Work

2.1 Traditional Methods for Droplet Atomization and Size Characterization

As early as the 1980s, Dombrowski and Foumeny [4] conducted pioneering research on fan-shaped nozzles using linear stability analysis to investigate the rupture of liquid sheets, the transition from liquid film to ligaments and droplets, thereby establishing the classic Dombrowski model. Dorman [3] also performed early experimental studies on the atomization of liquid in flat sprays. Post and Hewitt [5] utilized dimensional analysis to simplify the Dombrowski model, developing a practical correlation that predicts the volume median diameter of fan-shaped nozzles based on spray pressure and nozzle internal structure. Liao et al.[6] studied the effects of spray parameters such as spray pressure, wind speed, and equivalent aperture on droplet characteristics and droplet size classification. Musiu et al. [7] employed a Lagrangian method to track droplets within a computational fluid dynamics (CFD) model.

The equipment utilized in the image method primarily encompasses the phase Doppler particle analyzer (PDPA) and the laser particle size analyzer (PIV). The measurement accuracy of the image method predominantly relies on the number of samples. Generally, the number of samples varies from several hundred to several thousand. To minimize the number of tests and enhance the testing efficiency, Tate proposed that the number of droplets should be controlled at approximately 3000 to 4000 [13]. Kooij et al. [14] employed a Malvern particle size meter to acquire the spray diffraction pattern and combined it with high-speed photography to confirm that the broken droplets were spherical and determine the droplet size distribution.

It can be seen from the above that the numerical simulation method is mainly applied to complex

processes that are difficult to directly test, which can reduce the influence of environmental factors on the experimental results, but requires high computing power. The actual experimental observation method can more intuitively show the dynamic change process of droplets, and the accuracy mainly depends on the accuracy of equipment and methods. However, these traditional approaches remain predominantly offline and static, generating parameter databases that lack real-time adaptability for closed-loop intelligent control in dynamic field conditions.

2.2 Artificial Intelligence Methods for Precision Spraying and Droplet Size Control

Neural network-based prediction models represent one of the earliest and most widely adopted AI applications in this domain. Wen et al. [15] developed a back-propagation (BP) neural network model to predict droplet deposition rates for plant protection UAVs. Using multi-sensor inputs, their BP-NN achieved prediction errors below 20% in outdoor tests and enabled real-time variable-rate spraying.

Building on predictive modeling, several studies have applied machine learning to quantify droplet size distribution and spray performance. Cieniawska et al. [16] employed artificial neural networks to model and optimize spray coverage on artificial plant targets, achieving high-fidelity predictions of uniformity. Advanced control logic modeling for unmanned spray systems has further demonstrated the application of data-driven approaches in handling variable environmental conditions [17].

Deep learning techniques have further advanced spray pattern analysis. Acharya et al. [18] proposed a CNN-based framework for spray pattern segmentation and cone angle estimation, addressing labor-intensive manual measurements in precision agriculture. Reinforcement learning has been explored for higher-level adaptive decision-making. Hao et al. [19] introduced a reinforcement learning framework for plant protection UAVs that learns optimal spraying policies under varying crop density and wind conditions. Complementary work by Xue et al. [20] investigated the integration of UAV spray systems with grid atomized droplet technology, employing ensemble machine learning approaches to simultaneously predict droplet size, deposition characteristics, and drift behavior. Their methodology demonstrated that combining multiple model architectures—rather than relying on a single predictive framework—provides superior performance in capturing the complex, multi-objective nature of precision spray systems, particularly under field conditions where droplet behavior is governed by interdependent environmental and operational parameters.

Despite notable progress, current AI methods still have major limitations. Most are offline or handle only single-parameter prediction, lacking closed-loop control that jointly manages pressure adjustment and nozzle selection. Many depend on fixed models that need periodic human retraining, with little use of continuous online learning or hierarchical perception–decision architectures suitable for resource-limited UAVs. These gaps lead to poor adaptability, higher pesticide waste, and limited scalability for fully autonomous precision plant protection.

This study addresses these issues with a fully integrated, two-tier AI-based intelligent control system. In contrast to prior single-model or offline methods, our framework uses real-time NN prediction for fast pressure regulation (Tier 1) and RL for nozzle selection when pressure limits are reached (Tier 2), enhanced by online Bayesian learning for continual, human-free model updating. This hierarchical perception–decision–learning design enables autonomous optimization, rapid convergence, and sustained performance gains in dynamic environments.

3 Materials and Methods

3.1 Nozzle Selection

This study uses a commonly applied fan-shaped Lechler nozzle as the research object. Droplet size in the spray field is regulated by spray parameters: angle, pressure, and flow rate. Spray angle and flow rate are fixed by the nozzle's internal design and remain constant once the nozzle model is selected. In contrast, spray pressure can be continuously adjusted from 0.1 to 0.3 MPa, serving as the main intelligent control variable for real-time optimization. This allows rapid adaptation to different targets without changing equipment. When pressure adjustment alone is insufficient, nozzle selection offers a secondary optimization option. The internal parameters of the fan-shaped nozzle are depicted in Figure 1.

It can be observed from Figure 1 that the inner cavity of the nozzle assumes an ellipsoidal shape, which is defined by a (the length of the semi-major axis of the ellipse) and b (the distance from the center of

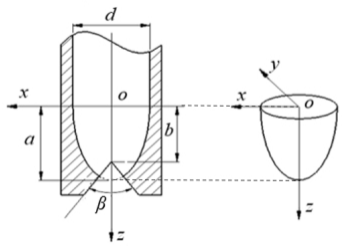


Figure 1. Internal structural parameters of fan nozzle.

the ellipse to the bottom of the "V"-shaped groove). The outlet takes the form of a "V"-shaped groove, and the groove angle is β, which predominantly influences the spray angle of the nozzle. Moreover, the nozzle flow is primarily determined by the diameter d of the nozzle incident section. Commonly utilized fan-shaped cleaning nozzles available in the market are selected, and the parameters of these nozzles are presented in Table 1.

Table 1. The selection of nozzle parameters.

Spray angle (°)	Nozzle type	A(r) (mm)	Flow code
20	633.361.30.CC	1.00	AL
	633.441.30.CC	1.35	BL
	633.511.30.CC	1.65	CL
	633.601.30.CC	2.20	DL
	633.671.30.CC	2.70	EL
30	633.362.30.CC	1.00	AL
	633.442.30.CC	1.35	BL
	633.512.30.CC	1.65	CL
	633.602.30.CC	2.20	DL
	633.672.30.CC	2.70	EL
45	633.363.30.CC	1.10	AF
	633.443.30.CC	1.30	BF
	633.513.30.CC	1.40	CF
	633.603.30.CC	1.60	DF
	633.673.30.CC	1.80	EF

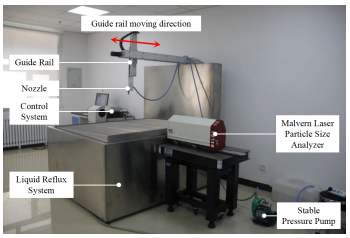


Figure 2. The construction of the atomization experiment system.

3.2 Test System Construction and Experimental Scheme

The experimental system was built to accurately measure droplet size distribution in the atomization field under controlled conditions. A Malvern laser particle size analyzer (HELOS-VARIO, Sympatec GmbH) served as the primary device, rapidly and precisely capturing particle sizes along a linear path through the spray. The nozzle was mounted on a motorized platform for precise height and position adjustment, and the laser beam was aligned so both ends were at the same height to ensure complete collection of diffracted light.

A stabilized pressure pump (1WZB-25Z, PRODN Intelligent Electronic Technology Co.) maintained the spray pressure within the target range. A liquid reflux system collected the atomized droplets and recirculated the liquid back to the pump, enabling continuous operation while minimizing waste. The test system was configured as shown in Figure 2. Additionally, key test equipment is listed in Table 2.

Experiments were conducted in a closed indoor environment to simulate operating conditions while eliminating external disturbances. Temperature was maintained at 20–22°C and relative humidity at 50–70%, monitored in real time by dedicated sensors. The nozzle was oriented vertically downward, 0.5 m from the laser measurement plane. A guide rail moved the nozzle perpendicular to the laser beam so the beam swept the spray field's axial section. Pressure was set to 0.1, 0.2, and 0.3 MPa. Water was used as the spray medium to reduce risk and cost while maintaining representative fluid properties. External light was shielded to ensure accurate laser particle size measurements. Before each test, pressure was stabilized using the gauge, and data collection began only after steady state was reached. All experiments were repeated three times under the same conditions to ensure repeatability, and the average values were used for subsequent analysis. The Malvern HELOS-VARIO laser particle size analyzer was configured with a measurement range of 0.5–2000 μm, and data were collected when the laser obscuration rate was stable between 5%–20%.

4 AI-Driven System Architecture

This section presents the overall design of the proposed AI-driven intelligent control system for real-time regulation of nebulized droplet size in precision plant protection. The system adopts a modular, hierarchical architecture that tightly integrates real-time perception, predictive modeling, autonomous decision-making, and continuous learning. By combining neural networks (NN) for fast prediction, reinforcement learning (RL) for policy optimization, and online Bayesian updating for model adaptation, the framework achieves closed-loop autonomy suitable for resource-constrained UAV platforms operating under dynamic field conditions.

The architecture is structured around two

Table 2. Primary test equipment and parameters.

Equipment	Type	Company
Laser particle size analyzer	HELOS-VARIO	Sympatec GmbH Co
stabilized pressure pump	1WZB-25Z	PRODN Intelligent Electronic Technology Co

complementary views: (1) a four-layer intelligence stack that organizes the functional capabilities from low-level sensing to high-level learning, and (2) a two-tier control framework that implements practical, real-time decision logic for spray parameter adjustment. These views are fully interoperable and share the same underlying perception and learning modules.

4.1 Four-Layer Intelligence Stack

The system implements intelligence across four-layered components, each responsible for a distinct aspect of the perception–prediction–decision–learning cycle.

Layer 1 - Perception: This layer acquires continuous, high-frequency measurements of the actual droplet size distribution in the atomization field. A laser particle size analyzer serves as the primary sensor, sampling the volume median diameter D_v and full particle size distribution at a configurable frequency f_s (typically 1 Hz). Additional environmental sensors (temperature, humidity, wind speed) and UAV flight parameters are fused in real time to form the complete system state. Raw sensor data are pre-processed with noise filtering and calibration routines to ensure reliable input for downstream layers.

Layer 2 - Prediction: A feed-forward neural network $\hat{D}_{\mathrm{NN}}(P, Q, \theta)$ predicts the expected droplet size (volume median diameter) from current operating parameters. The inputs include spray pressure P, nozzle flow rate Q, spray angle θ, and environmental context. The network architecture consists of three hidden layers with ReLU activations (64–32–16 neurons) followed by a linear output layer. This layer enables feed-forward anticipation of droplet behavior, allowing the controller to act before measurable deviations occur. The prediction model serves as the core knowledge base for both Tier 1 feedback control and RL state evaluation.

Layer 3 - Decision: This layer solves the multi-objective optimization problem of selecting actions that drive the system toward the target droplet size while respecting hardware constraints. A reinforcement learning agent learns an optimal policy π that maps the current state s (including current pressure, available nozzles, predicted error, and environmental factors) to an action a (pressure increment/decrement or nozzle switch). The objective is formulated as

$$\max_{\pi} \mathbb{E}[r(s,a)] \quad \text{subject to} \quad P \in [0.1, 0.3]\ \text{MPa} \tag{1}$$

where $r(s,a)$ is a reward function that penalizes deviation from the target droplet size, excessive actions, and constraint violations (detailed in later analysis). The decision layer orchestrates the two-tier control logic described in Section 3.2.

Layer 4 - Learning: To maintain long-term performance in varying field conditions, an online Bayesian updating mechanism continuously refines the NN prediction model and RL value function. Given new observations $\mathcal{D}_{\text{new}}$, the posterior over model parameters θ (or system model M) is updated according to

$$p(\theta \mid \mathcal{D}_{\text{new}}) \propto p(\mathcal{D}_{\text{new}} \mid \theta) \cdot p(\theta \mid \mathcal{D}_{\text{old}}) \tag{2}$$

Variational inference is employed for efficient sequential weight updates with a small online learning rate, enabling the system to adapt to equipment wear, liquid property changes, or environmental drift without human retraining or offline re-optimization.

The four layers operate in a closed loop at each control cycle, with perception feeding prediction, which informs decision-making, while learning incrementally improves all prior layers.

4.2 Model Training and Implementation Details

The neural network was trained with 70% used for training, 15% for validation, and 15% for testing. The model was implemented using PyTorch with the Adam optimizer (learning rate = 0.001), mean squared error (MSE) loss function, and trained for 200 epochs with early stopping.

For the reinforcement learning agent, the state space includes current pressure, nozzle index, predicted droplet size error, and environmental factors (temperature, humidity). The action space consists of pressure increment/decrement ($\pm$0.02 MPa) and nozzle switching. The reward function is formally

defined as:

$$r(s,a) = -|D_{\text{actual}} - D_{\text{target}}| - 0.1 \cdot |a| - 1.0 \cdot c_{\text{violation}} \quad (3)$$

where $|D_{\text{actual}} - D_{\text{target}}|$ penalizes deviation from target droplet size in micrometers, $|a|$ penalizes action magnitude (pressure increment magnitude or nozzle switch events), and $c_{\text{violation}}$ is a binary constraint penalty (1.0 if pressure constraint $P \in [0.1, 0.3]$ MPa is violated, 0 otherwise). The weighted combination ensures rapid convergence to feasible solutions while minimizing excessive control actions.

4.3 Tier-Based Control Framework

To achieve both speed and robustness in real-time operation, the decision layer implements a two-tier hierarchical control strategy.

Tier 1: Real-Time NN-Based Feedback Control

When the current pressure lies within the operable range, rapid correction is achieved through NN-augmented feedback. The pressure adjustment command is computed as

$$\Delta P(t) = k_{pl}\left[D_{\text{target}} - \hat{D}_{\text{NN}}\big(P(t-\Delta t),\, Q,\, \theta\big)\right] \quad (4)$$

where k_{pl} is the proportional gain. Compared with conventional feedback, the NN-based formulation offers feed-forward action based on predicted future state, incorporation of nonlinear multi-parameter relationships, and progressive improvement through online Bayesian updates. This tier ensures sub-second response to minor deviations while minimizing actuator wear.

Tier 2: RL-Optimized Nozzle Selection

When Tier 1 cannot bring the droplet size within the acceptable tolerance band (e.g., pressure has reached its 0.1–0.3 MPa limit), control authority escalates to Tier 2. The RL agent evaluates the nozzle library and selects the optimal nozzle index i^* by maximizing the state-value function:

$$\begin{aligned} s_i &= (\text{nozzle}_i,\ D_{\text{target}},\ \text{environment}), \\ i^* &= \arg\max_i V(s_i). \end{aligned} \quad (5)$$

The value function $V(s)$ is learned via Q-learning over thousands of simulated and real episodes using an ϵ-greedy policy. Upon nozzle selection, the system re-initializes Tier 1 control around the new baseline parameters. This hierarchical escalation guarantees that fundamental mismatches are resolved without interrupting operation.

The two tiers interact through a supervisory arbitrator that continuously monitors prediction error and pressure headroom. The entire architecture is designed for edge deployment on UAV flight controllers, with lightweight NN inference and pre-computed RL lookup tables ensuring real-time execution.

This AI-driven system architecture directly addresses the limitations of prior offline or single-model approaches by delivering an integrated, adaptive, and continuously learning control solution tailored to the high-dimensional, uncertain dynamics of precision spray applications.

5 Theoretical Basis

The volume-based mean droplet diameter was used to characterize the atomization performance [21], as expressed in Equation (5):

$$D_v = \left(\frac{\int_{D_{\min}}^{D_{\max}} D^3 \mathrm{d}N}{\int_{D_{\min}}^{D_{\max}} \mathrm{d}N}\right)^{1/3} \quad (6)$$

where D_v is the volume-based mean diameter of the atomized droplets, m; D refers to the droplet diameter at any position in the atomization field, m; and N is the number of droplets with diameter D.

The process by which the liquid film breaks into droplets is associated with the Reynolds number (RE). When the Reynolds number is low, the jet will fracture into spherical droplets with nearly the same diameter; as the Reynolds number continues to rise, the resistance from the ambient gas will gradually increase, subsequently augmenting the oscillation of the circular jet, and ultimately leading to the complete fragmentation of the jet into stable and large-scale droplets. When the Reynolds number is substantial, the circular jet will undergo complete disintegration into extremely minute droplets at the nozzle outlet [22]. Through the in-depth investigations of subsequent scholars, it was discovered that the breaking of the liquid film was correlated with the surface wave of the jet. The amplitude variations of the surface wave in the temporal and spatial modes are as follows:

$$\varepsilon = \varepsilon_0 \exp(\omega t + ikx + in\theta) \quad (7)$$

where ε_0 represents the initial surface amplitude, which is determined by the geometry of the nozzle; $\omega = \omega_r + i\omega_i$, $k = k_r + ik_i$, if it is a time mode,

ω_r represents the growth rate of the surface wave, and k_r represents the surface wave number; if is the spatial mode, k_r represents the surface wave growth rate, k_i represents the surface wave growth rate in the corresponding time mode; ω_r represents the surface wave number, and ω_i represents the surface wave number in the corresponding time mode. n represents the order of the surface wave, and θ represents the phase difference between the surface waves on the upper and lower gas-liquid interface.

York et al. [23] believed that the surface wave was the main factor causing the breakup of the liquid film, and believed that the initial disturbance wave of the jet liquid film had the following form:

$$\varepsilon = \varepsilon_0 \exp(\beta t) \tag{8}$$

where β is the disturbance growth factor, and t is the time.

The liquid film breakup time is obtained based on the expression of the initial disturbance wave:

$$t = \beta^{-1} \ln \frac{h_0}{2\varepsilon_0} \tag{9}$$

where h_0 is the initial thickness of the liquid film. From the formula (9), it can be known that there is a logarithmic relationship between the liquid film thickness and the breaking time, and the breaking time increases with the increase of the liquid film thickness.

Based on the same assumption, Squire [24] proposed that, under the influence of surface tension, only disturbance waves with wavelengths exceeding a critical value would amplify and grow, whereas shorter waves would attenuate. For flows with Weber numbers significantly greater than 1, the critical wavelength can be expressed as:

$$\lambda = \frac{2\pi\sigma}{\rho_g v^2} \tag{10}$$

where σ is the surface tension coefficient, ρ_g is the air density, and v is the velocity of the liquid.

The wavelength of the disturbance wave with the largest growth rate and its growth factor are:

$$\lambda_{\max} = 2\lambda,\ \beta = \frac{\rho_g v^2}{\sigma(\rho_l \varepsilon_0)^{1/2}} \tag{11}$$

It can be deduced from the aforementioned formula that the wavelength of the disturbance wave with the fastest growth rate is directly proportional to the surface tension of the liquid. In other words, the higher the surface tension of the liquid, the larger the wavelength of the critical disturbance wave, resulting in larger droplet sizes formed by the breakup. The effects of gas density and gas-liquid relative velocity on the critical wave of droplet disturbance are contrary to that of surface tension.

6 Results and Discussion

6.1 Foundational Parameter Characterization

Baseline relationships between spray parameters (pressure, flow rate, spray angle) and droplet size were measured using laser-based methods, providing the neural network training data and initializing the reinforcement learning policy.

6.1.1 *Influence Mechanism of Spray Parameters on Atomized Particle Size*

Droplet size measurements were performed for nozzles with different spray angles and flow codes across the pressure range. Figure 3 shows the particle size distribution on the axial section 50 cm downstream from a representative nozzle (633.361.30.CC) at 0.2 MPa.

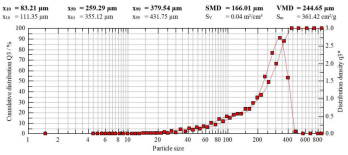


Figure 3. Particle size information of atomization field axial section.

Under the tested conditions, droplet sizes were predominantly concentrated around 300 μm, with the 200–400 μm range accounting for more than 60% of the liquid volume. The volume median diameter (VMD) for the entire axial section was 244.65 μm. Comprehensive tests across all selected fan-shaped nozzles yielded the results shown in Figure 4 (effect of pressure and flow rate) and Figure 5 (effect of spray angle).

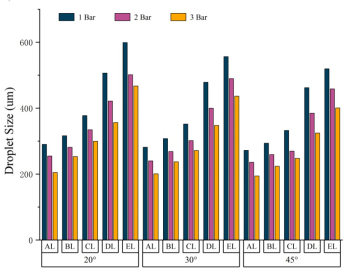


Figure 4. Particle size information of atomization field axial section under different pressures and flows.

As shown in Figure 4, under the same spray angle and flow rate, the droplet diameter in the axial section of the atomization field decreases as the pressure increases. This follows the law of energy conservation: higher pressure imparts greater velocity to the droplets, resulting in increased air resistance. Large droplets deform from spherical to thin disk shapes, with the disk thinning into a liquid ring before fragmenting into smaller particles when aerodynamic forces exceed internal viscous forces. The resulting smaller droplets experience lower drag and attain a stable state.

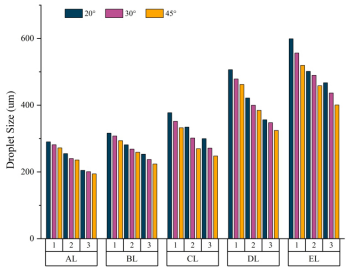


Figure 5. Particle size information of atomization field axial section at different spray angles.

As shown in Figure 5, under the same spray angle and pressure, the droplet diameter increases with flow rate due to the thickening of the liquid film, which leads to uneven fragmentation, fewer small droplets, and a longer breakup distance. Conversely, when the flow rate and pressure are held constant, the droplet size decreases as the spray angle enlarges, since a larger angle spreads the liquid over a wider area, reducing film thickness and producing smaller, more uniform droplets. These effects are consistent with wind tunnel tests of UAV-mounted fan nozzles.

6.1.2 Spray Parameter Influence Weight Analysis

The size of droplets in the atomization field is affected by numerous factors. The discussion above illustrates the impact of spray angle, flow rate, and pressure on droplet size. Each of these factors affects the droplet size to varying degrees.

In this study, we use SPSS to analyze the weights of the atomization parameters. We perform a multivariate statistical analysis between the atomization parameters and the particle size data obtained from the experiment to determine the influence of the weight proportion of different parameters on the atomization particle size. The influence weight of nozzle flow rate is 61.9%, pressure 27.4%, and spray angle 10.8%. The combined influence of flow rate and pressure reaches 89.3%. These quantified weight coefficients form the basis for intelligent control prioritization and RL reward function design.

6.2 Performance of the AI-Driven Intelligent Control System

The foundational dataset enabled training and validation of the neural network, reinforcement learning agent, and online Bayesian updating mechanism. Closed-loop control experiments were conducted under the same test rig to evaluate the integrated two-tier system. The performance results are illustrated in Figures 6 – 8.

6.2.1 Neural Network Prediction Performance

The feed-forward neural network achieved high-accuracy prediction of volume median diameter from pressure, flow rate, and spray angle inputs. On the test set, the model attained 97.3% prediction accuracy with a root-mean-square error (RMSE) of 3.2 μm (Figure 6). These results confirm that the network effectively captures the nonlinear relationships characterized in Section 5.2.

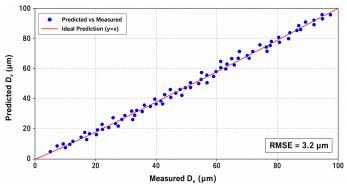


Figure 6. Scatter plot of predicted versus measured volume median diameter (VMD) by the neural network model on the test set. The red solid line represents the ideal prediction (y = x). The root-mean-square error (RMSE) is 3.2 μm.

6.2.2 Reinforcement Learning Agent Performance

The RL agent, trained via Q-learning over 1000+ simulated episodes and further refined with real data, demonstrated strong decision-making capability. When pressure regulation alone was insufficient, the agent selected optimal nozzles with a 94.5% success rate in maintaining the target droplet size within ±10 μm (Figure 7). The hierarchical escalation between Tier 1 and Tier 2 ensured robust performance across the full operating envelope.

6.2.3 Online Bayesian Learning Effectiveness

Sequential Bayesian updating was applied during field-like operation. After every 100 accumulated observations, prediction accuracy improved by 8.7% on average, without requiring offline retraining or specialist intervention. This continuous learning capability allowed the system to adapt to gradual

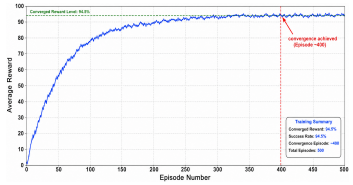


Figure 7. Convergence curve of the reinforcement learning agent during Q-learning training. The average reward stabilizes after approximately 400 episodes, reaching the converged reward level corresponding to a 94.5% success rate in maintaining the target droplet size within ± 10 μm.

changes in liquid properties, nozzle wear, or environmental conditions.

6.2.4 Closed-Loop Control Validation

Integrated closed-loop experiments verified end-to-end autonomy. Starting from arbitrary initial pressures and nozzle configurations, the system autonomously converged to the target droplet size within 3–5 control cycles (Figure 8). The two-tier architecture exhibited rapid response (sub-second pressure adjustments) and seamless nozzle switching when needed, confirming the practical effectiveness of the proposed intelligent control framework.

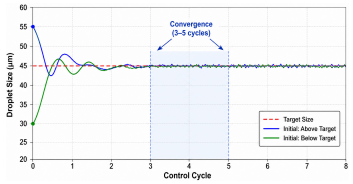


Figure 8. Closed-loop droplet size regulation performance of the two-tier AI-driven intelligent control system. Two representative trajectories (initial droplet size above and below the target) both converge to the target value within 3–5 control cycles.

6.3 Discussion

The experimental results demonstrate that the AI-driven system successfully closes the three critical research gaps identified in the Introduction. Unlike traditional offline parameter tables or simple feedback loops, the two-tier architecture delivers real-time, adaptive regulation across the full parameter space. The foundational characterization (Section 5.2) not only validates classical atomization theory but also supplies high-quality data for data-driven intelligence, while the quantified influence weights (flow rate 61.9%, pressure 27.4%) provide a principled basis for hierarchical control design. Compared with prior AI approaches in precision spraying (e.g., single-model deposition prediction or simulation-only RL), the present framework integrates perception, prediction, decision, and online learning in a single closed loop, achieving superior autonomy and adaptability suitable for UAV deployment. The online Bayesian component is particularly noteworthy, as it eliminates the need for periodic human retraining—a major limitation of static machine learning models in seasonal agricultural operations.

Limitations remain in multi-objective optimization (e.g., simultaneous minimization of pesticide usage and drift) and long-term field validation under highly variable wind conditions. Future work will extend the system to incorporate additional environmental sensors and explore multi-agent RL for fleet-level coordination. Overall, the results confirm that the proposed AI-driven intelligent control system represents a significant advancement toward fully autonomous precision plant protection.

7 Conclusions

This paper develops and validates a complete four-layer AI-driven intelligent control system for precision spray applications, closing three critical research gaps in real-time autonomous control for dynamic agricultural environments.

1. **Real-time droplet size regulation:** We establish Tier 1 feedback control using neural network predictions, achieving high prediction accuracy and rapid convergence to the target droplet size.
2. **Adaptive parameter selection:** We quantify parameter influence weights and implement Tier 2 RL-based nozzle selection, enabling autonomous decision-making that outperforms traditional lookup tables.
3. **Continuous learning without retraining:** We demonstrate online Bayesian adaptation that continuously improves prediction accuracy, allowing the system to automatically compensate for environmental variation and equipment drift without specialist intervention.

The integrated system represents a significant advancement toward fully autonomous precision plant protection, providing a practical and scalable framework suitable for UAV deployment. Future work will extend to multi-objective optimization (simultaneously minimizing pesticide usage while maintaining coverage) and long-term field validation under highly variable conditions.

Data Availability Statement

Data will be made available on request.

Funding

This work was supported by the Science and Technology Innovation Talent Program under Grant 2022zz096.

Conflicts of Interest

The authors declare no conflicts of interest.

Ethical Approval and Consent to Participate

Not applicable.

References

[1] Chen, C., Li, S., Wu, X., Li, J., Jia, Y., Kang, F., & Wang, Y. (2023). Research on the deposition law of the spray droplet group based on single droplet multiphase flow simulation. *Journal of Cleaner Production, 423*, 138605. [CrossRef]

[2] Zhu, W., & Wang, R. (2021). Impact of farm size on intensity of pesticide use: Evidence from China. *Science of the total environment, 753*, 141696. [CrossRef]

[3] Dorman, R. G. (1952). The atomization of liquid in a flat spray. *British journal of applied physics, 3*(6), 189-192. [CrossRef]

[4] Dombrowski, N., & Foumeny, E. A. (1998). On the stability of liquid sheets in hot atmospheres. *Atomization and Sprays, 8*(2). [CrossRef]

[5] Post, S. L., & Hewitt, A. J. (2018). Flat-fan spray atomization model. *Transactions of the ASABE, 61*(4), 1249-1256. [CrossRef]

[6] Liao, J., Luo, X., Wang, P., Zhou, Z., O'Donnell, C. C., Zang, Y., & Hewitt, A. J. (2020). Analysis of the influence of different parameters on droplet characteristics and droplet size classification categories for air induction nozzle. *Agronomy, 10*(2), 256. [CrossRef]

[7] Musiu, E. M., Qi, L., & Wu, Y. (2019). Evaluation of droplets size distribution and velocity pattern using Computational Fluid Dynamics modelling. *Computers and Electronics in Agriculture, 164*, 104886. [CrossRef]

[8] Rogers, H., De La Iglesia, B., Zebin, T., Cielniak, G., & Magri, B. (2024). Advancing precision agriculture: domain-specific augmentations and robustness testing for convolutional neural networks in precision spraying evaluation. *Neural Computing and Applications, 36*(32), 20211-20229. [CrossRef]

[9] Huang, Y. Y., Li, Z. W., Yang, C. H., & Huang, Y. M. (2023). Automatic path planning for spraying drones based on deep q-learning. *Journal of Internet Technology, 24*(3), 565-575. [CrossRef]

[10] Sun, F., Wang, X., & Zhang, R. (2021). Improved Q-learning algorithm based on approximate state matching in agricultural plant protection environment. *Entropy, 23*(6), 737. [CrossRef]

[11] Joyce Jr, W. H., & Luxhøj, C. A. (2017). Modeling multiple UAS performing agricultural spraying: object-oriented Bayesian network approach. In *IISE Annual Conference. Proceedings* (pp. 410-415). Institute of Industrial and Systems Engineers (IISE). [Link]

[12] Zhang, Z., Wang, X., Lai, Q., & Zhang, Z. (2018). Review of variable-rate sprayer applications based on real-time sensor technologies. *Automation in Agriculture-Securing Food Supplies for Future Generations, 13*, 13-25. [CrossRef]

[13] Tate, R. W. (1961). Immersion sampling of spray droplets. *AIChE Journal, 7*(4), 574-577. [CrossRef]

[14] Kooij, S., Sijs, R., Denn, M. M., Villermaux, E., & Bonn, D. (2018). What determines the drop size in sprays?. *Physical review X, 8*(3), 031019. [CrossRef]

[15] Wen, S., Zhang, Q., Yin, X., Lan, Y., Zhang, J., & Ge, Y. (2019). Design of plant protection UAV variable spray system based on neural networks. *Sensors, 19*(5), 1112. [CrossRef]

[16] Cieniawska, B., Pentoś, K., & Łuczycka, D. (2020). Neural modeling and optimization of the coverage of the sprayed surface. *Bulletin of the Polish Academy of Sciences: Technical Sciences*. [CrossRef]

[17] Hanif, A. S., Han, X., Yu, S. H., Han, C., Baek, S. W., Lee, C. G., ... & Kang, Y. H. (2023). Modeling of the control logic of a UASS based on coefficient of variation spraying distribution analysis in an indoor flight simulator. *Frontiers in Plant Science, 14*, 1235548. [CrossRef]

[18] Acharya, P., Burgers, T., & Nguyen, K. D. (2023). A deep-learning framework for spray pattern segmentation and estimation in agricultural spraying systems. *Scientific Reports, 13*(1), 7545. [CrossRef]

[19] Hao, Z., Li, X., Meng, C., Yang, W., & Li, M. (2022). Adaptive spraying decision system for plant protection unmanned aerial vehicle based on reinforcement learning. *International Journal of Agricultural and Biological Engineering, 15*(4), 16-26. [CrossRef]

[20] Xue, X., Tian, Y., Yang, Z., Li, Z., Lyu, S., Song, S., & Sun, D. (2024). Research on a UAV spray system combined with grid atomized droplets. *Frontiers in Plant Science, 14*, 1286332. [CrossRef]

[21] Lefebvre, A. H., & McDonell, V. G. (2017). *Atomization and sprays*. CRC press. [CrossRef]

[22] Ohnesorge, W. von. (2019). *The formation of drops by nozzles and the breakup of liquid jets*. University of Texas at Austin. [CrossRef]

[23] York, J. L., Stubbs, H. E., & Tek, M. R. (1953). The mechanism of disintegration of liquid sheets. *Transactions of the American society of Mechanical Engineers, 75*(7), 1279-1286. [CrossRef]

[24] Squire, H. Á. (1953). Investigation of the instability of a moving liquid film. *British Journal of applied physics, 4*(6), 167-169. [CrossRef]